U.S. DEPARTMENT OF THE INTERIOR

GEOLOGICAL SURVEY

A NOTE ON TRANSIENTS IN THE SRO AND ASRO LONG-PERIOD DATA

by
Jon Peterson

Open-File Report 82-702
1982

Data users have occasionally observed pulse-like transients in the long-period waveforms recorded at the Seismic Research Observatories (SRO) and at the Modified High-Gain Long-Period (ASRO) stations. In a recent paper, Dziewonski *et al* (1981) reported transients associated with earthquake signals recorded at some SRO stations, and the authors ascribed these transients to an unpredictable nonlinear system response. While some transients in the SRO and ASRO data are indeed generated by a nonlinear response (clipping), others are the result of linear processes. All event-associated transients are predictable in the sense that they are produced by large impulsive body-wave signals.

One type of transient occasionally observed in the long-period data is shown in Figure 1. In this example neither the seismometer nor the electronics have been overdriven and the system is presumably operating within its linear range. Transients of this type are often observed in the ASRO long-period data as well; an example is shown in Figure 2. The transients appear in both the vertical- and horizontal-component waveforms, although, in the case of teleseisms, horizontal-component amplitudes are generally much smaller (as in Figure 1.).

A second type of long-period transient is observed when the sensor system is operating beyond its linear range; an example is shown in Figure 3. In the SRO system short- and long-period signals are derived from a broadband signal generated by a single sensor. It is not possible, in the case of body waves, to accurately judge the level of the broadband signal by observing the long-period waveform. When long-period SRO data are being used in the analysis of body waves, it is advisable to check the short-period signal. If the short-period signal amplitude is 2,000,000 digital counts (2,000 digital counts for GUMO, SNZO, and TATO) or if the signal is distorted, the sensor system has been overdriven. This is the case for the example shown in Figure 3.

Another type of transient in the SRO long-period data, shown in Figure 4, occurs at regular intervals. The 25-second period steady-state signals in this figure are produced by a calibrating force applied to the inertial mass of each sensor. Long-period calibrations are made every day at 0 hours GMT. On every fifth day, at 5 minutes past 0 hours GMT, a 1-Hz sinusoidal signal is applied

to the sensor calibration circuit for a period of 1 minute in order to calibrate the short-period channel, and this produces the long-period transients appearing between the fifth and seventh minutes in Figure 4.

A fourth type of transient appears at random intervals in both the SRO and ASRO long-period data, although with much higher frequency in the ASRO data. An example is shown in Figure 5. In the case of the ASRO system, which uses conventional long-period seismometers, the cause is presumed to be mechanical dislocations in the instruments resulting from temperature changes. In the case of the SRO system, the pulses are usually observed simultaneously on the horizontal components, so the source is assumed to be external to the borehole seismometer, perhaps drops of condensation or settling of the holelock.

Impulse and step responses computed using the nominal SRO long-period transfer function are shown in Figure 6. Equivalent transient responses for the ASRO system are illustrated in Figure 7. Matching observed transients to the transients in this rogue's gallery of computed responses leads to some general conclusions concerning the transient behavior of the instruments, especially as to whether or not the observed process is linear.

For example, the long-period transients generated by the short-period calibration appear to be responses to impulses of earth acceleration (equivalent to a force acting on the mass, which results in mass displacement). The fact that this is indeed the case can be demonstrated by convolving a simulated calibration signal with the long-period acceleration impulse response. The result is compared in Figure 8 with the actual waveform recorded during a calibration. Since the transfer function used in the convolution is linear, one can infer that the long-period transient generated by a short-period calibration results from a predictable, linear process, not abnormal behavior of the instruments.

The long-period transients shown in Figures 1 and 2 are clearly similar in shape to the SRO and ASRO impulse responses to earth displacement. The similarity is illustrated in Figure 9, which shows the SRO impulse response to earth displacement overlaying the transient that appears in Figure 1. As one would expect, the convolution of an impulsive, earthquake-like signal with the SRO impulse response to earth displacement produces a similarly shaped

response (see Figure 10). The fact that we can reproduce this particular type of transient, which is the most common in the data, using a simulated earthquake signal and a linear transfer function would indicate that it results from a predictable, linear process and is not due to any misbehavior of the instrument.

The transient that occurs when the sensor is overdriven and the random transients that are believed to be caused by environmental disturbances are similar in appearance and closely match the shape of the step response to earth acceleration (see Figure 11b). This type of transient apparently results either from a permanent offset of the inertial mass caused by tilt or spring extension, or, in the case of the SRO system, from an electrical offset in the feedback circuit.

In conclusion, there are two identifiable classes of transients that appear in the SRO and ASRO data. One is an impulse response that results from a normal instrument response to an impulsive signal, and the other is a step response that either accompanies a nonlinear response to earth motion when the sensor is driven beyond its linear range or results from an environmental disturbance. Other than attempting better environmental control to reduce the number of random transients, there does not appear to be any way of eliminating the recording of long-period transients except by changing the system response. The long-period transients, which are largely shaped by the response of the long-period filters, would not appear in a broadband recording of the same waveform. However, if the broadband data containing an impulsive P arrival were filtered during analysis to bandpass the long-period signals, the long-period transient would reappear. The shape of the transients are highly predictable from the system transfer function. For some purposes, it may be appropriate and useful to subtract the transient from the waveform prior to analysis. This can be done quite effectively as illustrated in Figure 11b.

REFERENCE

Dziewonski, A.M., T.-A. Chou, and J.H. Woodhouse (1981). Determination of earthquake source parameters from waveform data for studies of global and regional seismicity, *J. Geophys. Res.*, *86*, 2825-2852.

ACKNOWLEDGMENT

The author wishes to thank Dr. George H. Sutton for reviewing this note and making helpful suggestions.

Figure Captions

Fig. 1. Short- and long-period waveforms recorded at the SRO station near Chiang Mai, Thailand from an m_b 6.0 earthquake at a depth of 599 kilometers. Distance to source is 89.8 degrees and azimuth is 290 degrees. The long-period transient was not clearly distinguishable on the north component.

Fig. 2. (a) Long-period waveforms recorded at the ASRO station near Kabul, Afghanistan from a local earthquake of unknown magnitude and location. (b) Impulsive, short-period signal that produced the long-period transients shown in (a).

Fig. 3. Vertical-component short- and long-period waveforms recorded at the Narrogin, Australia, SRO station from an m_b 6.0 earthquake at a depth of 200 kilometers. Distance to source is 49 degrees and azimuth is 238 degrees. The sensor system was clipped by the P arrival, as evident from the amplitude of the short-period signal.

Fig. 4. Waveforms recorded on an SRO system during long-period and short-period calibrations. The short-period calibration is applied to all three components, although only vertical-component short-period data are recorded.

Fig. 5. Random transients (unassociated with earthquake signals) recorded on the ASRO system at Kabul, Afghanistan.

Fig. 6. Long-period transient responses computed for the SRO system using the nominal transfer function (listed on the network-day tape).

Fig. 7. Long-period transient responses computed for the ASRO system using the nominal transfer function (listed on the network-day tape).

Fig. 8. Actual (left) and simulated (right) short- and long-period waveforms recorded on an SRO system during a short-period calibration. The simulated long-period waveform was derived by convolving the short-period calibration signal with the long-period earth acceleration impulse response.

Fig. 9. Long-period SRO impulse response to earth displacement overlaying the long-period transient shown for the vertical component in Figure 1.

Fig. 10. Simulated short- and long-period waveforms for an SRO system. The long-period waveform was derived by convolving the short-period signal with an impulse response to earth displacement.

Fig. 11. (a) Long-period SRO response to a step of earth acceleration overlaying the long-period transient shown in Figure 3. (b) Resulting waveform when the step response in (a) is subtracted from the recorded signal,

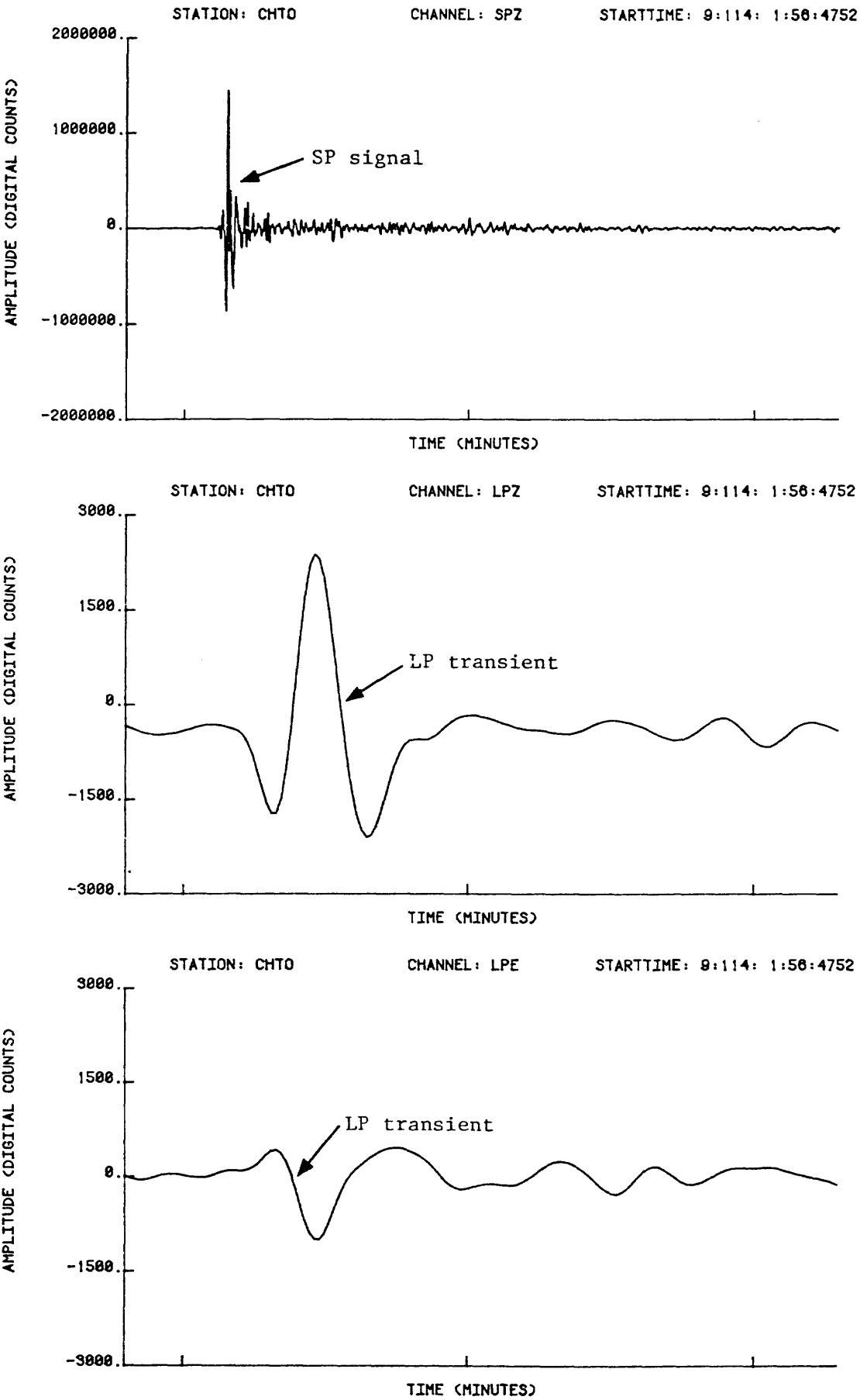
STATION: CHTO
CHANNEL: SPZ
STARTTIME: 9:114: 1:56:4752
2000000.
1000000.
0.
-1000000.
-2000000.
AMPLITUDE (DIGITAL COUNTS)
SP signal
TIME (MINUTES)
STATION: CHTO
CHANNEL: LPZ
STARTTIME: 9:114: 1:56:4752
3000.
1500.
0.
-1500.
-3000.
AMPLITUDE (DIGITAL COUNTS)
LP transient
TIME (MINUTES)
STATION: CHTO
CHANNEL: LPE
STARTTIME: 9:114: 1:56:4752
3000.
1500.
0.
-1500.
-3000.
AMPLITUDE (DIGITAL COUNTS)
LP transient
TIME (MINUTES)

FIG. 1.

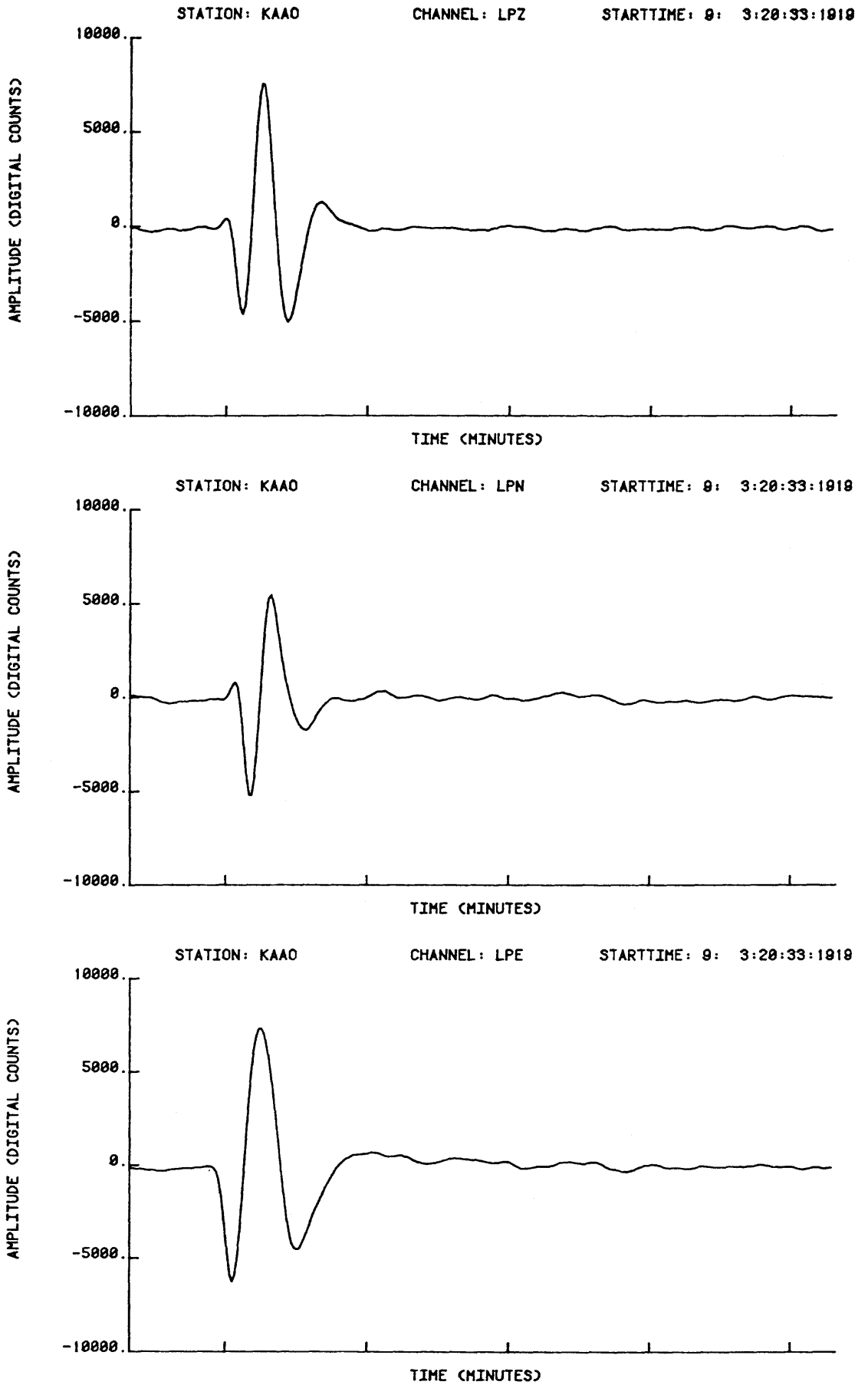
STATION: KAAO
CHANNEL: LPZ
STARTTIME: 0: 3:20:33:1919
10000.
5000.
0.
-5000.
-10000.
AMPLITUDE (DIGITAL COUNTS)
TIME (MINUTES)
STATION: KAAO
CHANNEL: LPN
STARTTIME: 0: 3:20:33:1919
10000.
5000.
0.
-5000.
-10000.
AMPLITUDE (DIGITAL COUNTS)
TIME (MINUTES)
STATION: KAAO
CHANNEL: LPE
STARTTIME: 0: 3:20:33:1919
10000.
5000.
0.
-5000.
-10000.
AMPLITUDE (DIGITAL COUNTS)
TIME (MINUTES)

FIG 2A.

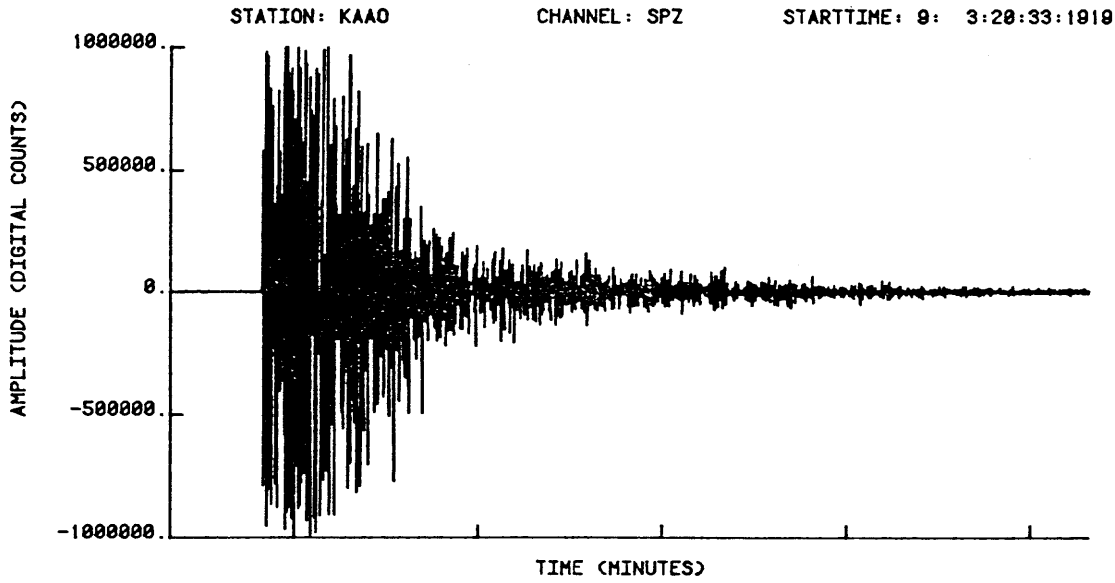
STATION: KAAO
CHANNEL: SPZ
STARTTIME: 9: 3:20:33:1919
1000000.
500000.
0.
-500000.
-1000000.
AMPLITUDE (DIGITAL COUNTS)
TIME (MINUTES)

FIG 2B.

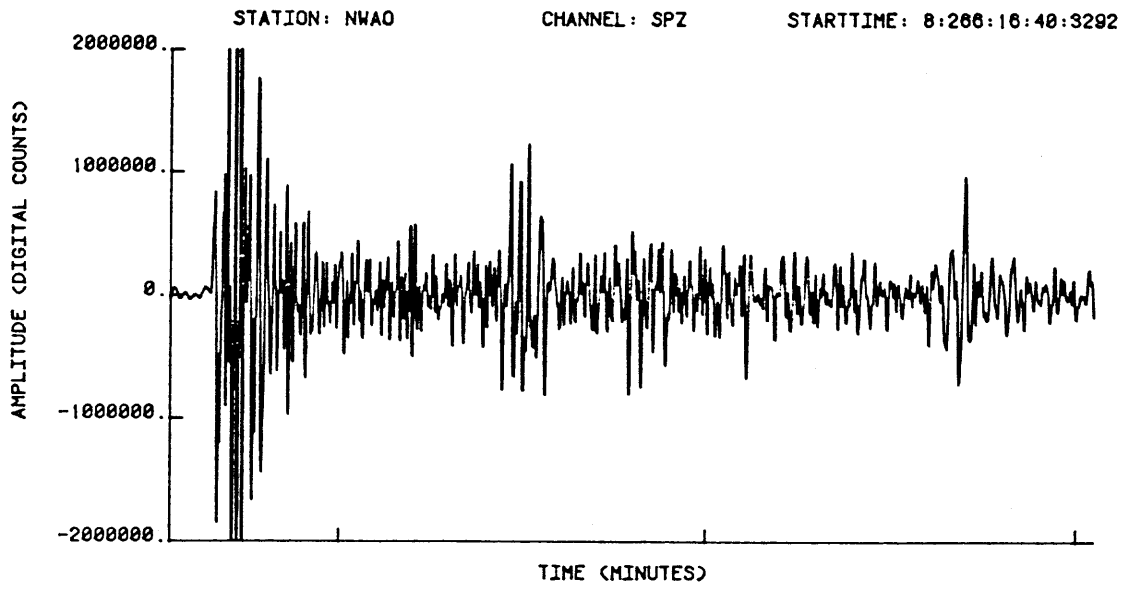
STATION: NWAO
CHANNEL: SPZ
STARTTIME: 8:266:16:40:3292
2000000.
1000000.
0.
-1000000.
-2000000.
AMPLITUDE (DIGITAL COUNTS)
TIME (MINUTES)

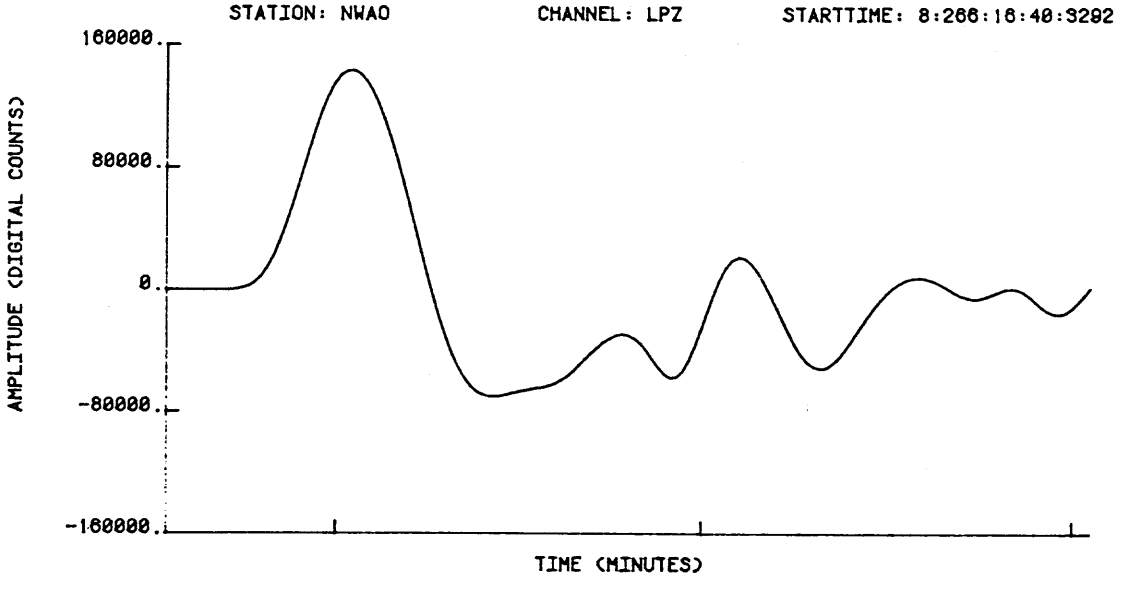
STATION: NWAO
CHANNEL: LPZ
STARTTIME: 8:266:16:40:3292
160000.
80000.
0.
-80000.
-160000.
AMPLITUDE (DIGITAL COUNTS)
TIME (MINUTES)

FIG 3.

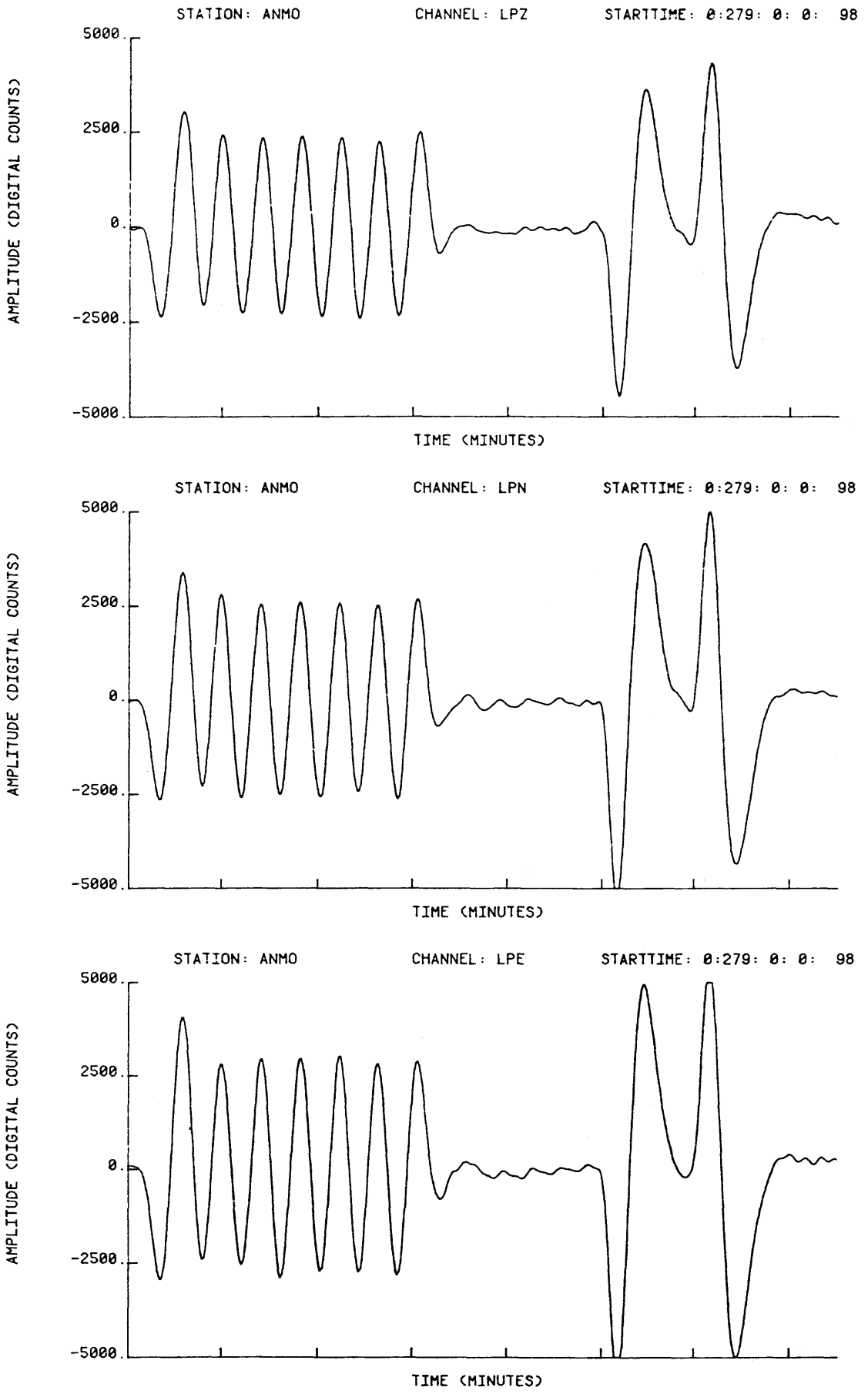
STATION: ANMO
CHANNEL: LPZ
STARTTIME: 0:279: 0: 0: 98
5000.
2500.
0.
-2500.
-5000.
AMPLITUDE (DIGITAL COUNTS)
TIME (MINUTES)
STATION: ANMO
CHANNEL: LPN
STARTTIME: 0:279: 0: 0: 98
5000.
2500.
0.
-2500.
-5000.
AMPLITUDE (DIGITAL COUNTS)
TIME (MINUTES)
STATION: ANMO
CHANNEL: LPE
STARTTIME: 0:279: 0: 0: 98
5000.
2500.
0.
-2500.
-5000.
AMPLITUDE (DIGITAL COUNTS)
TIME (MINUTES)

FIG 4.

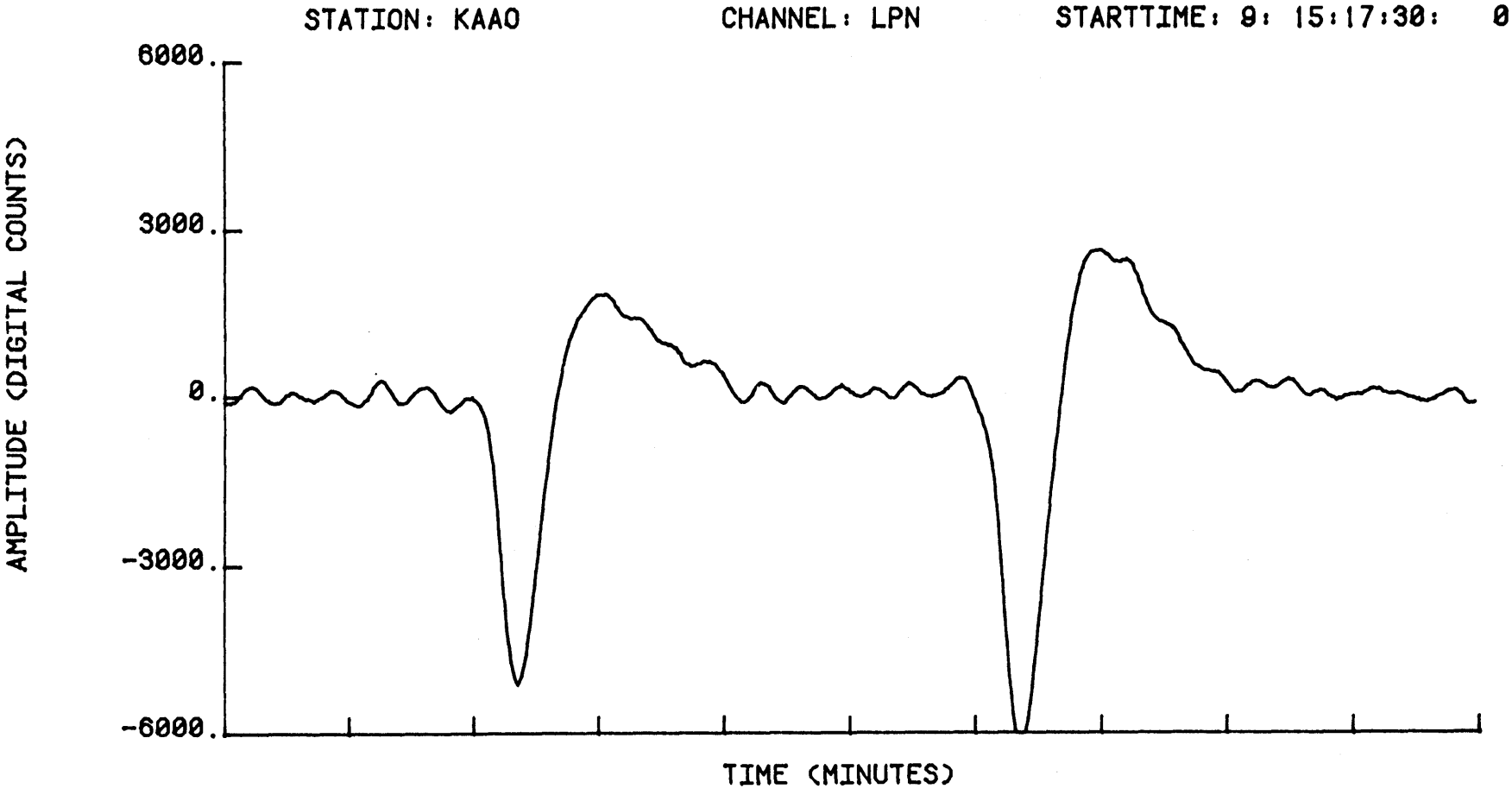
STATION: KAAO
CHANNEL: LPN
STARTTIME: 9: 15:17:30: 0
6000.
3000.
0.
-3000.
-6000.
AMPLITUDE (DIGITAL COUNTS)
TIME (MINUTES)

FIG 5.

EARTH DISPLACEMENT

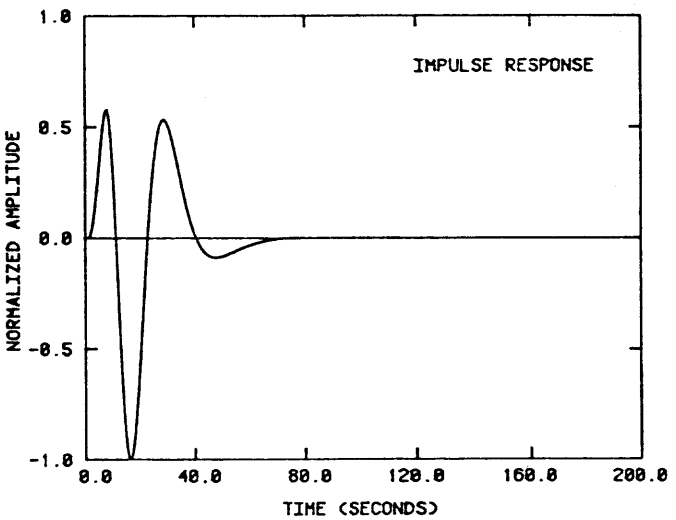

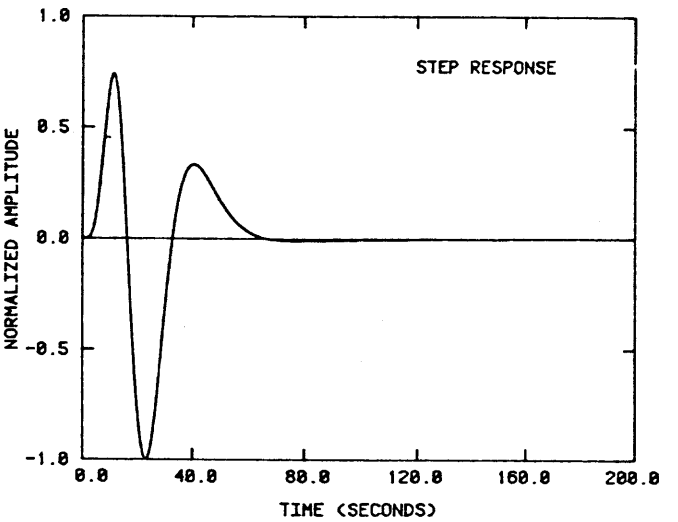

EARTH ACCELERATION

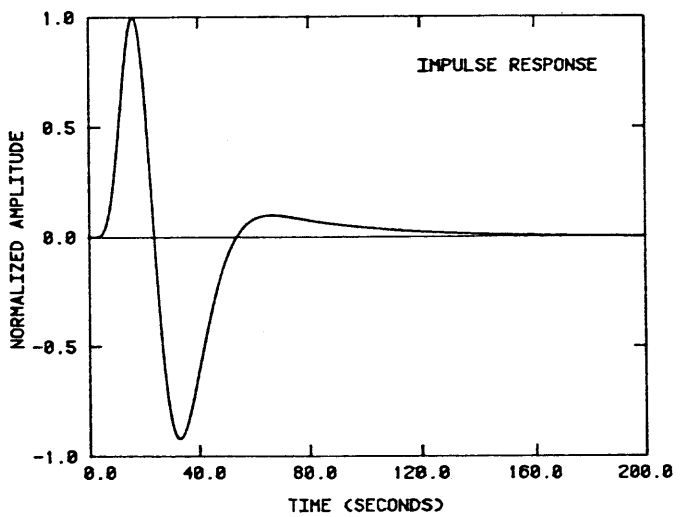

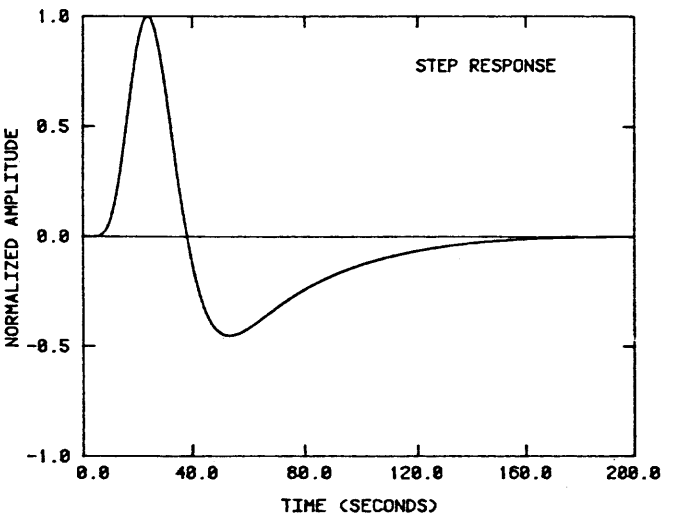

FIG 6.

EARTH DISPLACEMENT

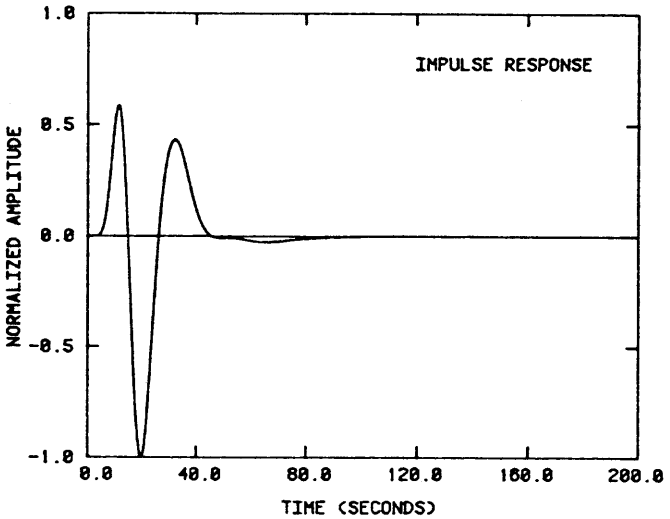

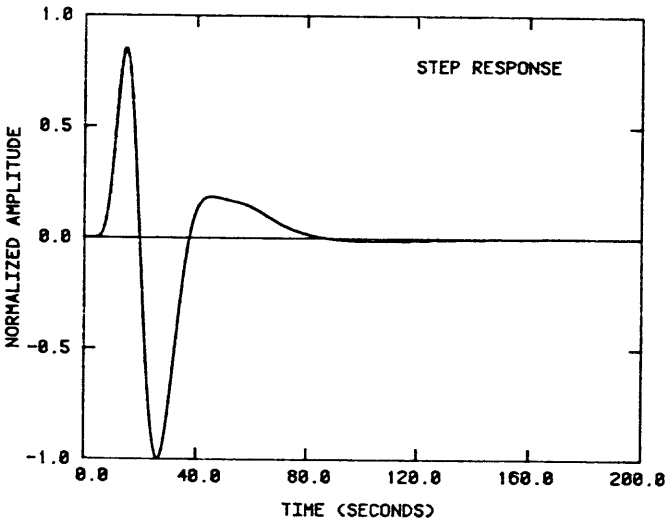

EARTH ACCELERATION

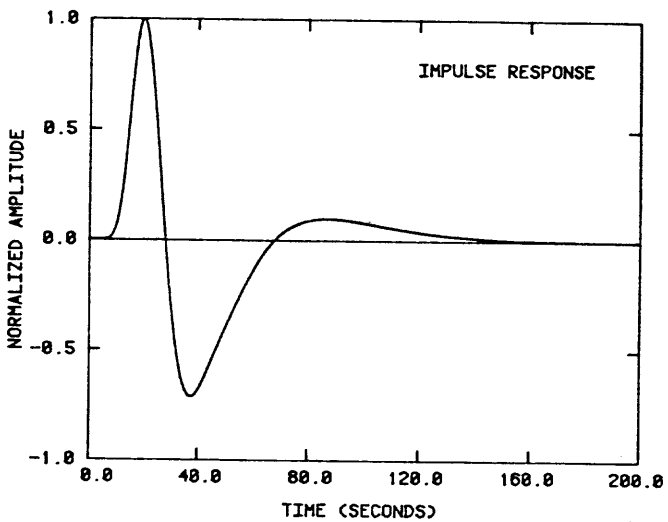

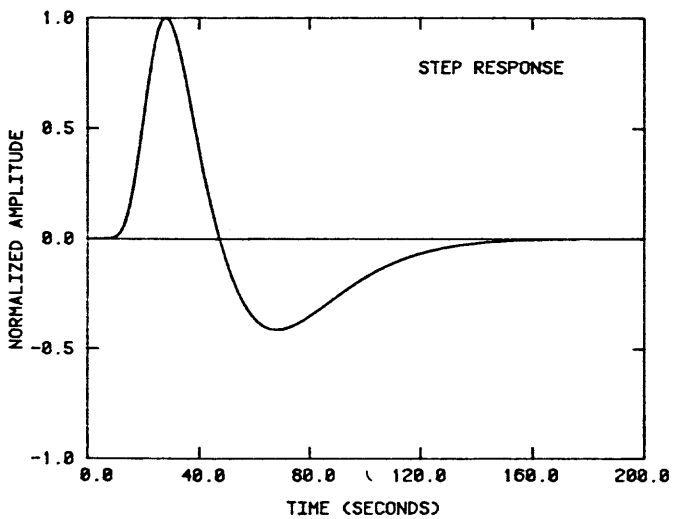

FIG 7.

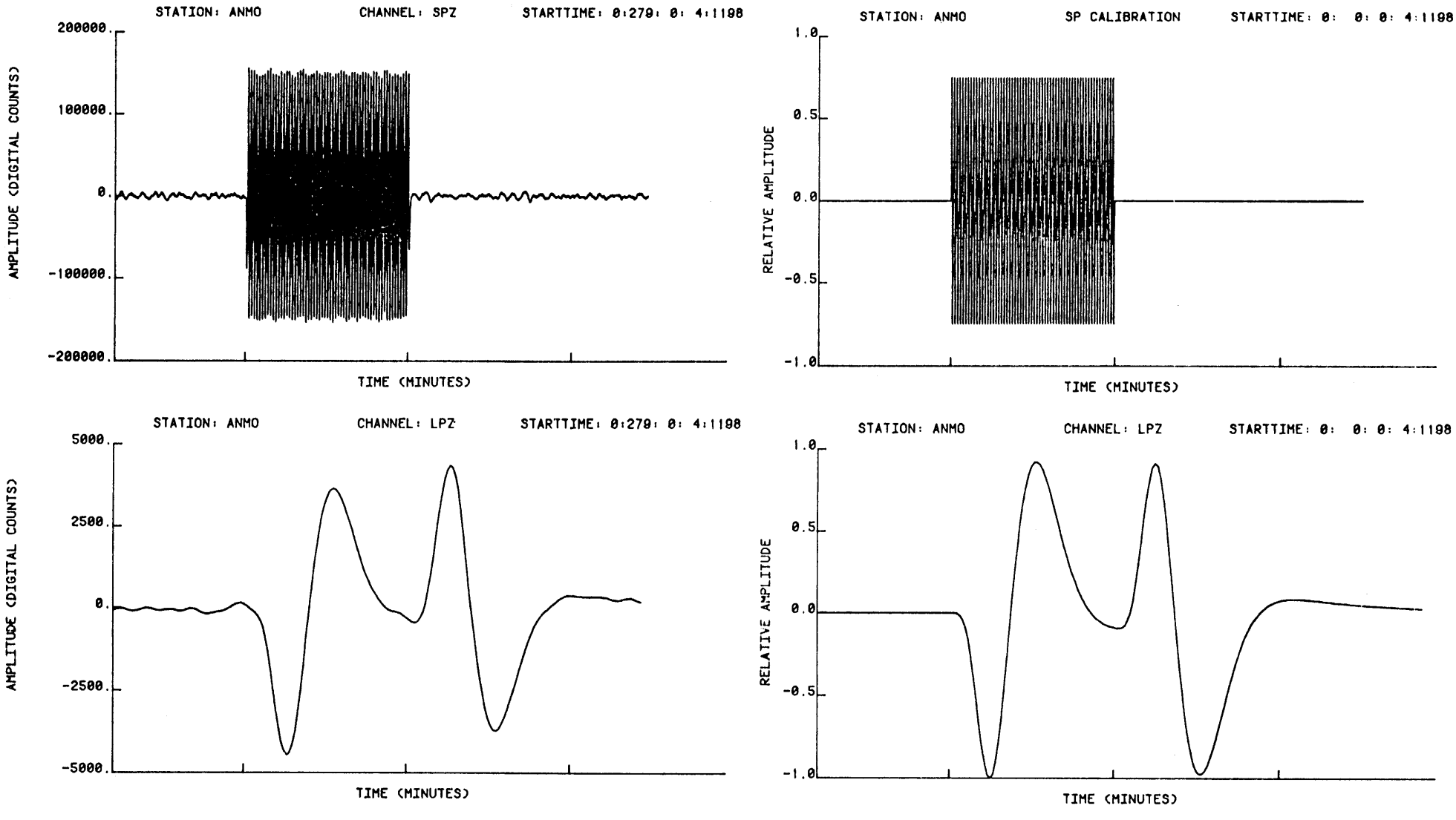
STATION: ANMO
CHANNEL: SPZ
STARTTIME: 0:279: 0: 4:1198
AMPLITUDE (DIGITAL COUNTS)
200000.
100000.
0.
-100000.
-200000.
TIME (MINUTES)
STATION: ANMO
SP CALIBRATION
STARTTIME: 0: 0: 0: 4:1198
RELATIVE AMPLITUDE
1.0
0.5
0.0
-0.5
-1.0
TIME (MINUTES)
STATION: ANMO
CHANNEL: LPZ
STARTTIME: 0:279: 0: 4:1198
AMPLITUDE (DIGITAL COUNTS)
5000.
2500.
0.
-2500.
-5000.
TIME (MINUTES)
STATION: ANMO
CHANNEL: LPZ
STARTTIME: 0: 0: 0: 4:1198
RELATIVE AMPLITUDE
1.0
0.5
0.0
-0.5
-1.0
TIME (MINUTES)

FIG 8.

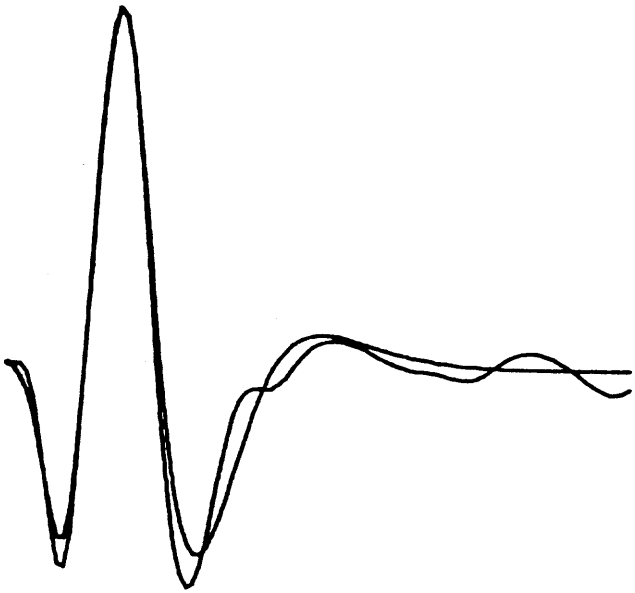

FIG 9.

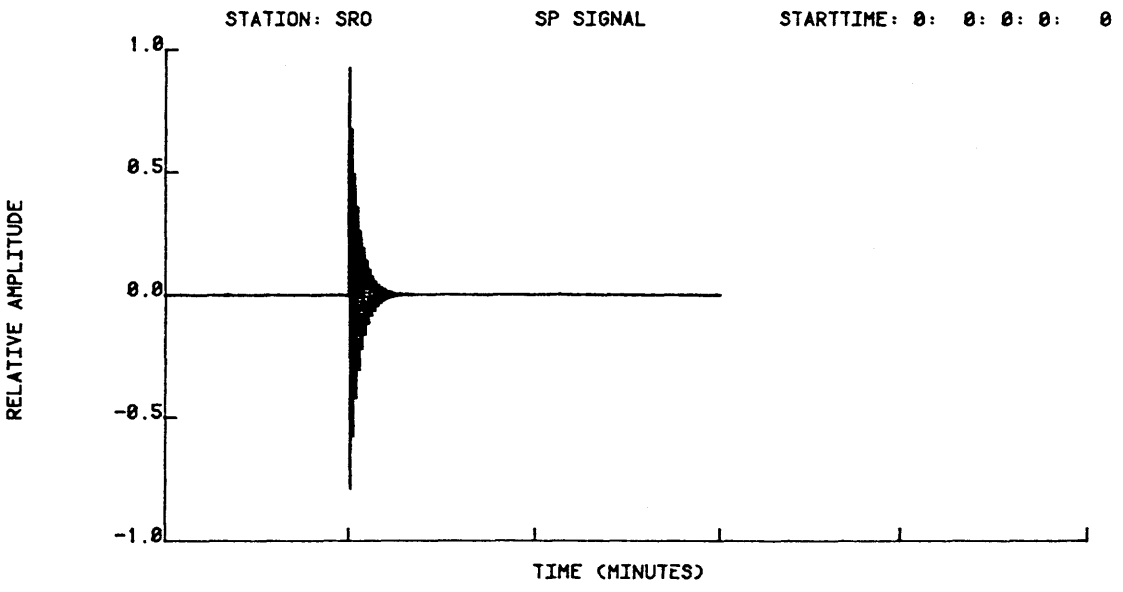
STATION: SRO
SP SIGNAL
STARTTIME: 0: 0: 0: 0: 0
1.0
0.5
0.0
-0.5
-1.0
RELATIVE AMPLITUDE
TIME (MINUTES)

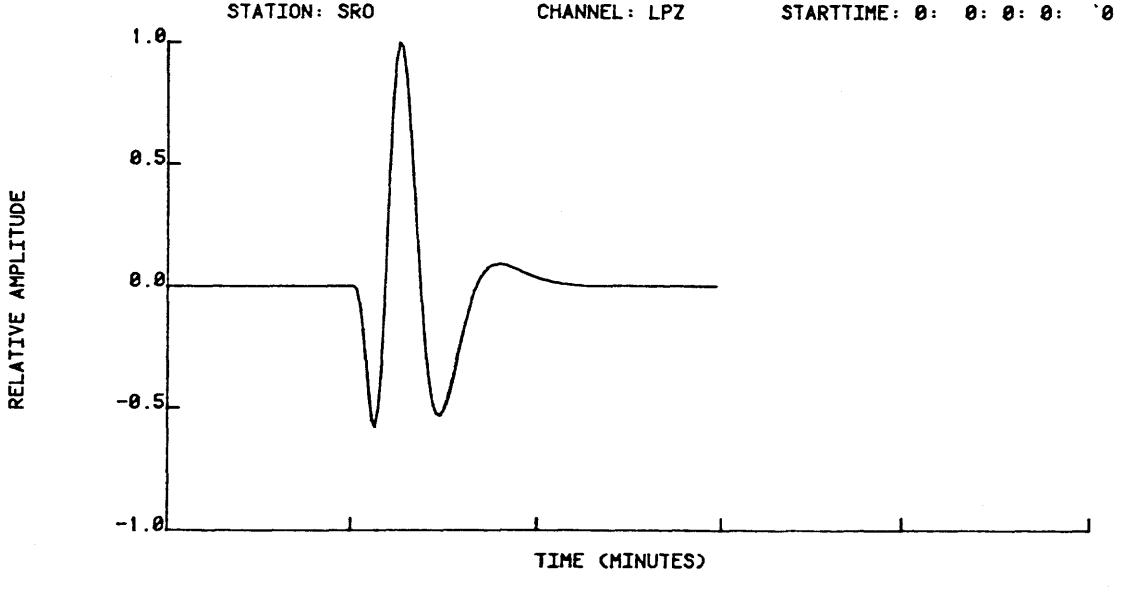
STATION: SRO
CHANNEL: LPZ
STARTTIME: 0: 0: 0: 0: 0
1.0
0.5
0.0
-0.5
-1.0
RELATIVE AMPLITUDE
TIME (MINUTES)

FIG 10.

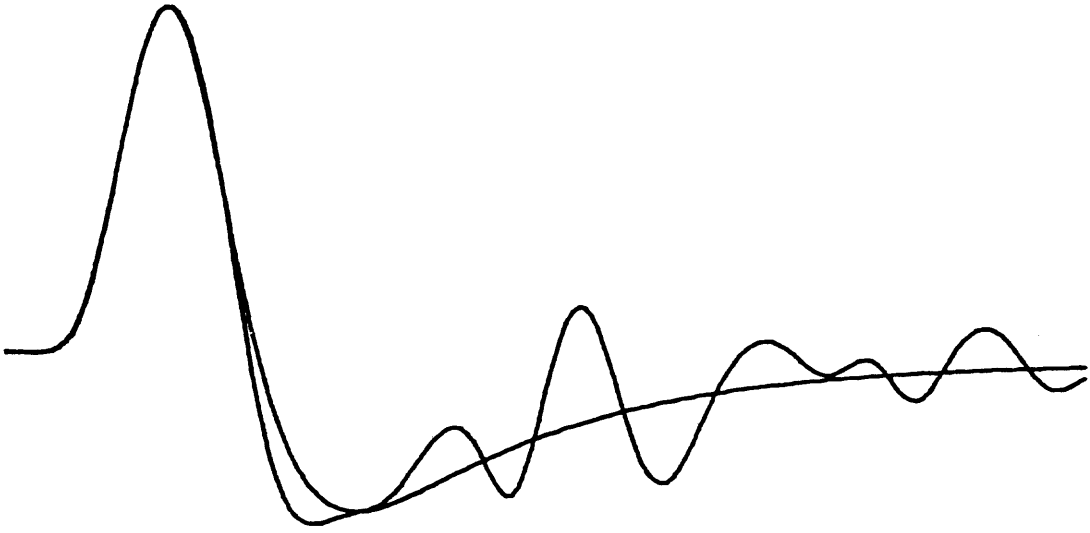

FIG 11A.

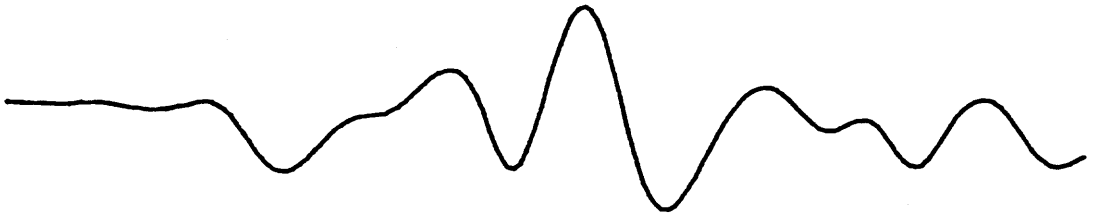

FIG 11B.